

Determination of Multipeak Textures with High-Energy Synchrotron Radiation

Andrea Preusser¹, Helmut Klein², Lars Raue² and Hans Joachim Bunge¹

¹Institute of Physics and Physical Technologies
Clausthal University of Technology, 38678 Clausthal-Zellerfeld, Germany.

²GZG, Department of Crystallography
University of Göttingen, 37077 Göttingen, Germany.

Keywords: Multipeak Textures, Moving Area Detector Method, ghost orientations, resolving power, pole figures, g-Matrices

Abstract. The 'Moving Area Detector Method' with high energy synchrotron radiation allows to measure textures and microstructures of materials with high location and orientation resolution, e.g. so called Multipeak Textures. In this paper the measuring method is described shortly, as well as a description and the calculation of Multipeak Textures are given. A few examples of synthetic calculated Multipeak pole figures are shown.

Introduction

In classical sense the texture of polycrystalline materials is a continuous function of three variables (e.g. Euler angles $\{\varphi_1 \Phi \varphi_2\}$) describing the crystal orientation g . This definition does not take into account individual crystallites and their positions $\{xyz\}$ in the sample. The most general description of the polycrystalline structure must specify the orientation $g\{xyz\}$ at any point in the material.

Texture development during recrystallization can be studied by X-Ray diffraction. With classical methods of texture measurements it is only possible to receive statistical distribution functions of many crystallites which cannot be distinguished individually. In order to understand the processes of recrystallization or grain growth, the behaviour of single crystallites must be known to follow their individual 'life path' during these processes.

Multipeak Textures

Multipeak Textures [2] consist of a large number (e.g. >100) of sharp and narrow peaks (e.g. $<1^\circ$). In this case a calculation of the Orientation Distribution Function with harmonic methods must provide an extremely high resolution. Using high resolved pole figures as input the problem has to be solved which pole figure peaks belong to the same crystal. Highest resolution in pole figures can be achieved by continuous imaging. The left side of figure 1 shows a 3D-section of an (111) pole figure measured with moving area detector method of a 93.3% cold rolled and recrystallized nickel sheet. Spots of individual recrystallized grains can be seen in an enlarged perspective representation. These grains are 'mounted' on the continuous 'ridge' of the deformation texture. The enlarged 2-D section of figure 1 shows individual spots. The detector pixel size of $150\mu\text{m}$ corresponds to $\sim 0.01^\circ$ and the half width (FWHM) of the spots

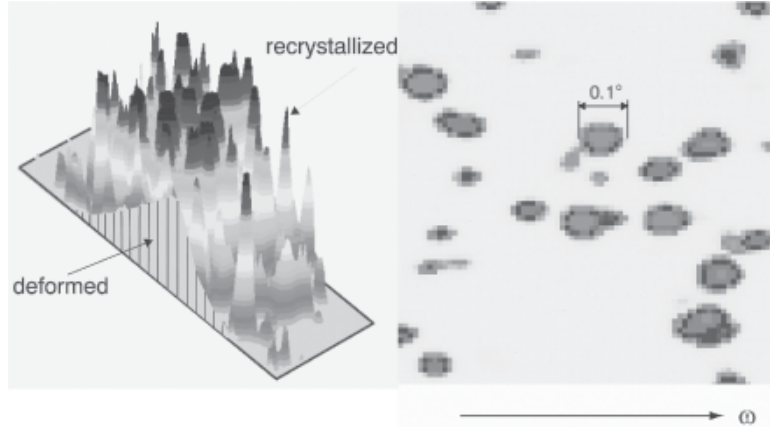


Fig. 1: Left: 3D-picture of an (111)-nickel pole figure. Right: Enlarged 2D-section

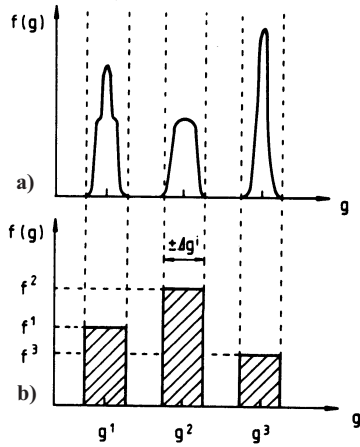


Fig. 2: Schematic (one-dimensional representation) of Multipole Textures.

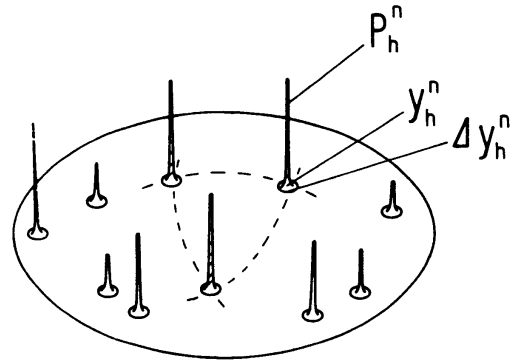


Fig. 3: Schematic illustration of pole figure peaks.

is in the order of 0.05° .

There are two levels of experimental resolving power Multipole Textures may be considered at. In the first case with high resolving power ($\Delta_{exp} \ll \Delta g^i$) the exact shape of the distribution function $f(g)$ within each spread range Δg^i is to be considered (Fig.2a). The orientation distribution in the vicinity of the peak orientation g^i may have different shapes as shown in figure. The density is zero except for a small environment Δg^i of certain peak orientations g^i . In the second case with moderate resolving power ($\Delta_{exp} \approx \Delta g^i$) the exact distribution is not considered (Fig.2b). Each orientation peak g^i is characterized by the spread range Δg^i , by the central position g^i and by the integrated density f^i . At the moment only the second case is assumed for further considerations. Figure 3 shows several peaks in a pole figure. The shape of the distribution function is not distinguished within each pole figure peak. The peaks exist of the integrated density P_h^n and the width Δy_h^n at the positions y_h^n , where h marks the type of the crystal plane and n is the peak number. The integrated density $P_n^{i,j}$ of a pole figure peak is related to the integrated density f^i in Euler space. That means, the pole figure peaks in the same pole figure belonging to the same orientation must have the same integrated density. Peaks belonging to the same orientation g^i cannot be initially distinguished from peaks belong-

ing to all other crystal orientations. So the main question is: Which values n belong to which orientation g' ?

Experimental Techniques

The structure of a polycrystalline material is characterized by the crystallographic orientation $g = \{\omega\gamma\psi\}$ in any small volume element at the location $x = \{xyz\}$ of the material. Hence, the six-dimensional orientation-location space $\{\omega\gamma\psi xyz\}$ must be imaged with highest possible resolution as available with synchrotron radiation [1]. In order to fully exploit the high resolving power of this radiation the conventional step-scan technique had to be replaced by a continuous 'sweeping' technique with a moving area detector [4]. For this purpose either a Bragg angle slit system [4] or a diffraction plane slit [4] was introduced additionally between sample and detector in the diffractometer at the high-energy beamline BW5 at HASYLAB/DESY Hamburg (Germany) (Fig. 4).

This technique allows to measure three types of two-dimensional images which are sections and projections of the six-dimensional orientation-location space. A rotation of crystal orientation through the angle ψ around the diffraction vector cannot be distinguished. Also the coordinate x along the incident beam remains unresolved in all three techniques. For multiphase textures the Bragg angle slit system is most important.

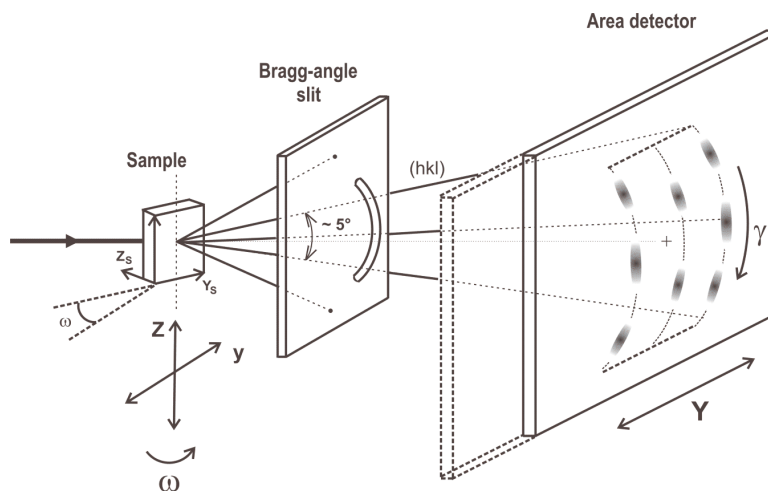


Fig. 4: Schematic figure of the Bragg angle slit system.

Examples In Figure 5 grain resolved rotation scans, obtained with Bragg angle slit, of a nickel sheet, cold rolled 93.3% and annealed for 3hrs at 873K are shown. Spots corresponding to [111] and [200] directions of individual grains can be seen. In high resolution {111} pole figures of the same nickel sheet (Fig. 6) single poles corresponding to individual recrystallized grains occur after 45 min annealing time (Fig. 6a). After 300min (Fig. 6b) the spots of the recrystallized grains tend to cumulate around the poles of the cube texture. Starting texture was the typical cold rolling texture. Non-measured areas are marked by dotted lines.

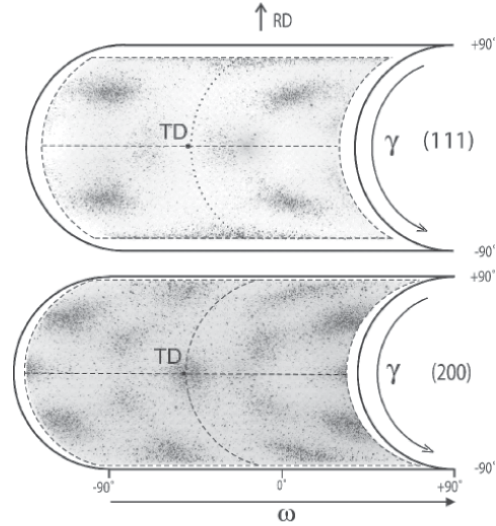


Fig. 5: Grain resolved rotation scan of a cold-rolled nickel-sheet, annealed for 3hrs at 873K.

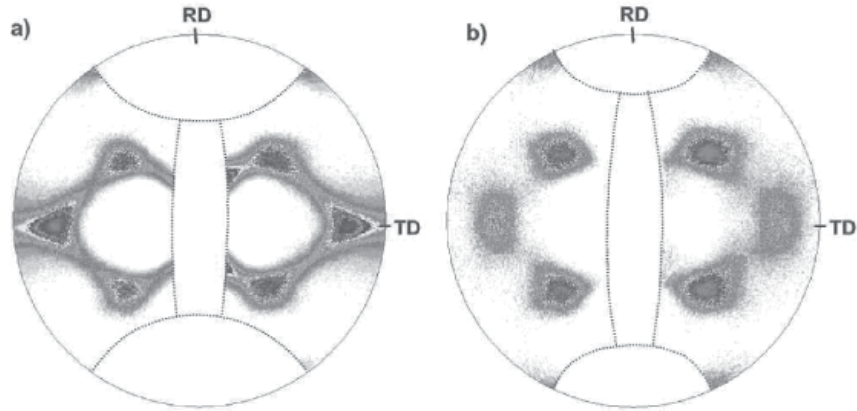


Fig. 6: Pole figures of a cold-rolled nickel-sheet, annealed for 3hrs at 873K, measured with Moving Area Detector Method. a) after 45min annealing time; b) after 300min annealing time.

Calculation of Multipeak Textures

The search procedure of the so called 'ODF' analysis for Multipeak Textures consists of two parts: (One has to keep in mind, that this procedure is no real 'ODF' analysis, because no orientation distribution function is calculated.)

1. A search procedure which has to find all real g^i (and possibly some 'ghost' peaks.)
2. The solution of $I_h^n = 4\pi \frac{m^c}{m_h} w_h \sum_{i=1}^N \lambda_i^n \cdot f^i$, which gives the volume fractions f^i of the orientations g^i and excludes ghosts.

where N is the total number of orientations g^i , m_h the number of different crystal directions and m^c the number of equivalent orientations. λ_i^n is equal one if i contributes to n and zero if i does not contribute to n . The equation contains two types of unknowns: First the normalization

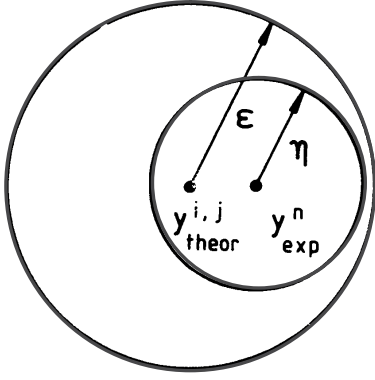


Fig. 7: The uncertainty η of experimentally determined peak positions y_{exp}^n and the tolerance circle ε around a theoretical position $y_{theor}^{i,j}$.

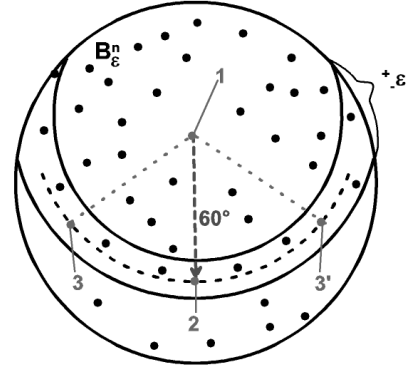


Fig. 8: Random poles in a (110) pole figure. Point 1 is chosen as the starting pole. Point 2 is found in a distance of $60^\circ \pm \varepsilon$. A third point must be found either at 3 or 3'.

factors w_h of the various pole figures and second the integrated densities f^i of the orientations g^i . The solution is now an iteratively one. In the first step w_h is approximated and the obtained solution for f^i is used to calculate w_h in the second step.

'Ghost' Orientations The peak positions are known only with the experimental accuracy η . Then the peak search procedure must accept peaks within a tolerance circle ε around the ideal position $y_{theor}^{i,j}$ (Figure 7). In order not to lose an orientation, the tolerance circle ε must be slightly larger than the uncertainty η . In this case it may happen that pole figure peaks belonging to different orientations are in the right position to fake an orientation g^i . This shall be called 'ghost' orientations (not to be mixed up with those of the Orientation Distribution Function).

The search procedure The uncertainty of the peak positions is $\eta \simeq \Delta_h^{i,j} + \Delta_{exp}$ with $\Delta_h^{i,j}$ as the natural peak width and Δ_{exp} as the resolving power. Now the search procedure must be able to find any orientation g^i . Therefore at least two poles are needed when there is a mirror plane if there is none, a third pole has to be found. That means for the (100) and (111) pole figures two neighbouring poles are enough, while for the (110) pole figure three neighbouring poles are needed. These two (or three) poles of any orientation are contained in the measured range B_h .

We choose the (110) pole figure to start. A starting pole plus a second peak belonging to the same orientation must be found in a distance of 60° (Fig. 8). Because of the experimental uncertainty the band $\pm \varepsilon$ must be considered to be possible counter parts to the peak 1. The probability for 'ghost' orientations can be reduced by looking for further poles of the same orientation within the measured range B_h of (110) and other pole figures. Only if all required poles are really found an orientation is accepted for being a possible orientation.

Examples

Figure 10 shows a theoretically random {111} pole figure with 30 crystallites (~ 120 {111} reflections). The open circles are the reflections of the randomly chosen orientations $\{\varphi_1 \phi \varphi_2\}$, while the grey circles illustrates the reflections obtained by the recalculated orientations. No experimental uncertainty η was chosen and the tolerance ε was assumed to be 0.1. The reflections of one orientation are shown as black points. One can see, that mostly all of the recalculated

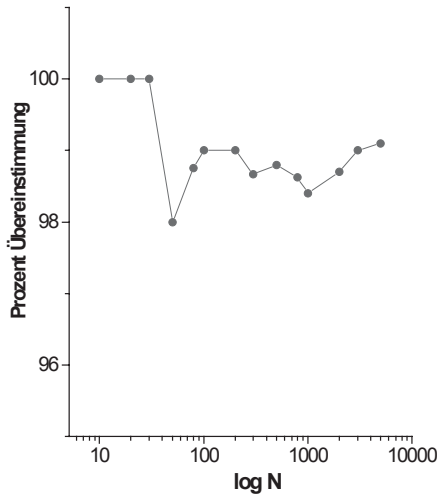


Fig. 9: Relationship between random number N and correspondence with the calculated values.

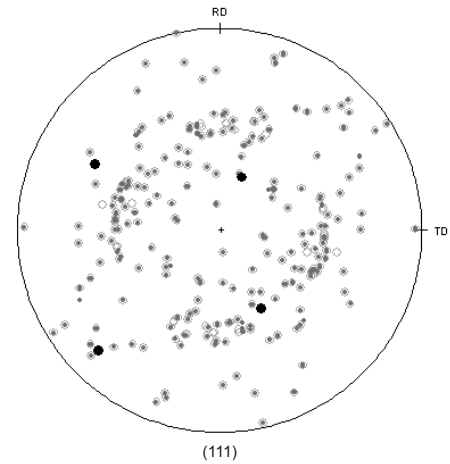


Fig. 10: (111) random pole figure.

reflections are in good agreement with the input values. The grey circles not surrounded by an open circle are 'ghost' reflections, open circles without a grey one were not found by the described search routine. For the discussion of the experimental data it is necessary to know more about the relationship between the number of input orientations and the number of agreements with the calculated values. This relationship between the input orientations N and the percentage of correspondence is illustrated in figure 9 for a number of orientations N up to 5000.

Acknowledgements

The authors gratefully acknowledge sponsoring this project, concerning Recrystallization and Multiphase Textures, by the German Research Foundation, DFG.

References

- [1] Bunge, H.J., Wcizlak,L., Klein, H., Garbe, U. and Schneider J.R.: *Advanced Engin Mater.* **4**, No.5 pp. 300-305 (2002)
- [2] Bunge, H.J., Morris, P.R. and Nauer-Gerhardt, C.U.: *Textures and Microstructures* **11** pp. 1-22 (1989)
- [3] H.J., Wcizlak,L., Klein, H., Bunge, H.J., Garbe, U., Tschentscher, T. and Schneider J.R.: *J. Appl. Crystallography* **35** pp. 82-95 (2002)
- [4] Bunge, H.J., Wcizlak,L., Klein, H., Garbe, U. and Schneider J.R.: *J. Appl. Crystallography* **36** pp. 1240-1255 (2003)
- [5] Klein, H. and Bunge, H.J.: *Z. Metallkunde* **90** pp. 103-110 (1999)
- [6] Bunge, H.J., Klein, H., Wcizlak,L., Garbe, U., Weiss W. and Schneider J.R.: *Textures and Microstructures* **35** pp. 253 (2003)

This article was processed using the L^AT_EX macro package with TTP style